

# Quantum chaos, thermalization and tunneling in an exactly solvable few body system

Shruti Dogra,<sup>1</sup> Vaibhav Madhok,<sup>1</sup> and Arul Lakshminarayan<sup>1</sup>

<sup>1</sup>*Department of Physics, Indian Institute of Technology Madras, Chennai, India 600036*

Exactly solvable models that exhibit quantum signatures of classical chaos are both rare as well as important - more so in view of the fact that the mechanisms for ergodic behavior and thermalization in isolated quantum systems and its connections to non-integrability are under active investigation. In this work, we study quantum systems of few qubits collectively modeled as a kicked top, a textbook example of quantum chaos. In particular, we show that the 3 and 4 qubit cases are exactly solvable and yet, interestingly, can display signatures of ergodicity and thermalization. Deriving analytical expressions for entanglement entropy and concurrence, we see agreement in certain parameter regimes between long-time average values and ensemble averages of random states with permutation symmetry. Comparing with results using the data of a recent transmons based experiment realizing the 3-qubit case, we find agreement for short times, including a peculiar step-like behaviour in correlations of some states. In the case of 4-qubits we point to a precursor of dynamical tunneling between what in the classical limit would be two stable islands. Numerical results for larger number of qubits show the emergence of the classical limit including signatures of a bifurcation.

In a modest pursuit of the esthetic attributed to Feller that “the best consists of the general embodied in the concrete” [1], we consider extreme quantum cases of the kicked top, a widely studied, text-book model of quantum chaos [2–4]. The general issues at hand are the emergence of the classical world from a quantum substratum and the role of quantum chaos in the thermodynamics of closed quantum systems [5–7]. Vigorous progress is being made in studying thermalization of isolated quantum systems that could be either time-independent or periodically forced [5–22]. Entanglement within many-body quantum states in such systems drives subsystems to thermalization although the full state remain pure and of zero entropy, see [20] for a demonstration with cold atoms.

Quantum chaos [3, 23] and, consequently, eigenstate thermalization hypothesis [7, 10] enables one to use individual states for ensemble averages. For periodically driven systems that do not even conserve energy, a structureless “infinite-temperature” ensemble emerges in strongly non-integrable regimes [15, 17]. A recent 3-qubit experiment, using superconducting Josephson junctions, that simulated the kicked top [19] (see also [24]) purported to remarkably demonstrate such a thermalization. Although such behavior has been attributed to non-integrability [7, 19], we exactly solve this 3-qubit kicked top, pointing out that it can be interpreted as a special case of an *integrable* model. Additionally we solve the 4-qubit case exactly, although there is no connection to an integrable model. The kicked top, in the limit of an infinite number of qubits displays a standard transition to Hamiltonian chaos and it is remarkable that many of the features are already reflected in the solvable few qubit cases.

For example, explicit formulas are obtained for entanglements generated and are compared, for the 3-qubit case, with data from the experiment in [19]. The infinite

time average of single qubit entanglement is found analytically for some initial states and at a special and large value of the forcing, for all initially unentangled coherent states. These are shown to tend to that obtained from relevant (random matrix) ensembles, in some cases even exactly coinciding with them and thus displaying thermalization. These demonstrate that even in the deep quantum regime, the transition to what in the classical limit becomes chaos is reflected in the time-averaged entanglement.

Naturally there are interesting quantum effects in these few-body systems. One, is the extremely slow convergence of subsystem entropies in the near-integrable regime that happens for some states of the 4-qubit case. Its origin is the presence of dynamical tunneling [25–29] between what appears in the classical limit as symmetric regular regions. In the near-integrable regime the exactly calculable tunneling splitting is shown to result in this long-time dynamics. This may open windows for experimental tests of the interplay of chaos, resonances and tunneling in systems with small number of qubits.

The quantum kicked top is a combination of rotations and torsions, the Hamiltonian [2–4] is given by  $H = (\kappa_0/2j)J_z^2 \sum_{n=-\infty}^{\infty} \delta(t - n\tau) + (p/\tau)J_y$ . Here  $J_{x,y,z}$  are components of the angular momentum operator  $\mathbf{J}$ . The time between periodic kicks is  $\tau$ . The Floquet map is the unitary operator  $\mathcal{U} = \exp[-i(\kappa_0/2j\hbar)J_z^2] \exp[-i(p/\hbar)J_y]$ , which evolves states just after a kick to just after the next. The parameter  $p$  measures rotation about the  $y$  axis, and in the following we set  $\hbar = 1$  and  $p = \pi/2$ .  $\kappa_0$  is the magnitude of a twist applied between kicks and controls the degree of chaos in the classical system. As the magnitude of the total angular momentum is conserved, the quantum number  $j$ , with eigenvalues of  $\mathbf{J}^2$  being  $j(j+1)\hbar^2$ , is a good one. The classical limit, when  $j \rightarrow \infty$  is a map of the unit sphere phase space  $X^2 + Y^2 + Z^2 = 1$

onto itself with the variables being  $X, Y, Z = J_{x,y,z}/j$  and is given by  $(X' = Z \cos(\kappa_0 X) + Y \sin(\kappa_0 X), Y' = -Z \sin(\kappa_0 X) + Y \cos(\kappa_0 X), Z' = -X)$ .

For  $\kappa_0 = 0$  the classical map is evidently integrable, being just a rotation, but for  $\kappa_0 > 0$  chaotic orbits appear in the phase space and when  $\kappa_0 > 6$  it is essentially fully chaotic. Connection to a many-body model can be made by considering the large  $\mathbf{J}$  spin as the total spin of spin=1/2 qubits, replacing  $J_{x,y,z}$  with  $\sum_{l=1}^{2j} \sigma_l^{x,y,z}/2$  [30, 31]. The Floquet operator is then that of  $2j$  qubits, an Ising model with all-to-all homogeneous coupling and a transverse magnetic field:

$$\mathcal{U} = \exp\left(-i \frac{\kappa_0}{4j} \sum_{l < l'=1}^{2j} \sigma_l^z \sigma_{l'}^z\right) \exp\left(-i \frac{\pi}{4} \sum_{l=1}^{2j} \sigma_l^y\right). \quad (1)$$

Here  $\sigma_l^{x,y,z}$  are the standard Pauli matrices, and an overall phase is neglected. The case of 2-qubits,  $j = 1$ , has been analyzed in [32] wherein interesting arguments have been proposed for the observation of structures not linked to the classical limit. For  $j = 3/2$ , the three qubit case is a nearest neighbor kicked transverse Ising model, known to be integrable [33, 34]. For higher values of the spin, the model maybe considered few-body realizations of non-integrable systems. In general only the  $2j + 1$  dimensional permutation symmetric subspace of the full  $2^{2j}$  dimensional space is relevant to the kicked top.

The initial states used are coherent states located at  $(X = \sin \theta_0 \cos \phi_0, Y = \sin \theta_0 \sin \phi_0, Z = \cos \theta_0)$  on the phase space sphere and given by  $|\theta_0, \phi_0\rangle = \otimes^{2j} (\cos(\theta_0/2)|0\rangle + e^{-i\phi_0} \sin(\theta_0/2)|1\rangle)$  [35, 36]. Note that for  $\kappa_0$  that are multiples of  $2\pi j$ ,  $\mathcal{U}$  is a local operator and does not create entanglement, we therefore restrict attention to the interval  $\kappa_0 \in [0, \pi j]$ . After time  $n$  the evolved state  $|\psi_n\rangle = \mathcal{U}^n |\theta_0, \phi_0\rangle$  is used to find the reduced density matrix  $\rho_1(n) = \text{Tr}_{\neq 1}(|\psi_n\rangle\langle\psi_n|)$ , obtained after tracing out all other spins except the first. As this is at most rank-2, the various entropies that depend on the eigenvalues alone are monotonic to each other and we use the simplest, the linear entropy  $S_{(\theta_0, \phi_0)}^{(2j)}(n, \kappa_0) = 1 - \text{Tr} \rho_1^2(n)$  as a measure of entanglement. Figure (1) shows the long-time average  $\langle S_{(\theta_0, \phi_0)}^{(3)}(\kappa_0) \rangle$  as a function of  $\kappa_0$ , for the case of 3-qubits, and three representative initial states. Each is seen to increase with the torsion  $\kappa_0$  either to  $1/3$  or a value close to it.

The average value of the linear entropy in the  $N$ -qubit permutation symmetric subspace is  $S_{RMT}(N) = (N - 1)/(2N)$  [37], and for  $N = 3$  this also gives  $1/3$ . For at least three particular initial states, with important classical phase space correspondences,  $|0, 0\rangle \equiv |000\rangle$  and  $|\pi/2, \pm\pi/2\rangle \equiv |\pm\pm\pm\rangle_y$  this value is, remarkably, exactly attained for  $\kappa_0 = 3\pi/2$ . For these states

$$\langle S_{(0,0)}^{(3)}(\kappa_0) \rangle = \frac{5 - 2s_0}{(4 - s_0)^2}, \quad \langle S_{(\frac{\pi}{2}, \pm\frac{\pi}{2})}^{(3)}(\kappa_0) \rangle = s_0 \frac{8 - 5s_0}{(4 - s_0)^2}, \quad (2)$$

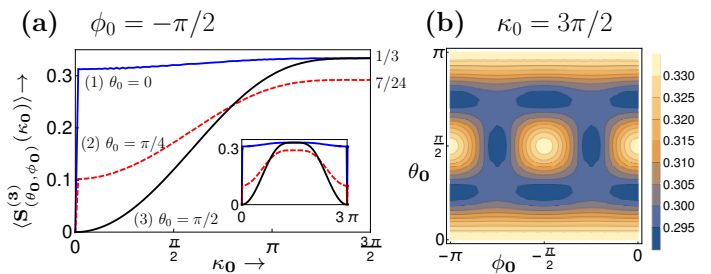


FIG. 1. (a) Time averaged linear entropy, obtained over  $n = 1000$  periods, of a single qubit vs the parameter  $\kappa_0$ , for three initial coherent states  $|\theta_0, \phi_0\rangle$ . The Eqs. (2) apply to the curves labeled (1) and (3), as for  $\theta_0 = 0$  the value of  $\phi_0$  is immaterial on the sphere. Inset shows the entanglement periodicity in the parameter at  $\kappa_0 = 3\pi$ . Part (b) displays the time averaged linear entropy across all initial coherent states for the value  $\kappa_0 = 3\pi/2$  and is described by Eq. (3).

with  $s_0 = \sin^2(\kappa_0/3)$  and  $\kappa_0 > 0$  (see below and [38]). While  $j = 3/2$  is too small to see effects such as the fixed points' loss of stability, the overall region surrounding the classical fixed points  $(\theta_0, \phi_0) = (\pi/2, \pm\pi/2)$  being stable for small  $\kappa_0$  and gradually losing stability as the parameter is increased is reflected in the gradual increase of average entropy corresponding to the initial states  $|\pi/2, \pm\pi/2\rangle$  starting from 0 when  $\kappa_0 = 0$ . Notice that from a purely quantum mechanical view,  $\otimes^{2j} |\pm\rangle_y$  are eigenstates of  $\mathcal{U}$  at  $\kappa_0 = 0$ . In contrast, the initial state  $|0, 0\rangle$  corresponds to a classical period-4 orbit and assumes entanglement entropy as large as  $5/16$  for arbitrarily small  $\kappa_0$ .

For the 3-qubit case, when  $\kappa_0 = 3\pi/2$ , the eigenvalues of  $\mathcal{U}$  are  $\exp(\pm 2\pi i/3)$  and  $\pm \exp(\pm \pi i/6)$ , implying that  $\mathcal{U}^{12} = I$ . Thus infinite time averages are finite ones over a period, in fact entanglement has a period of 6 in this case and for arbitrary initial coherent states, the time-averaged entanglement entropy is

$$\langle S_{(\theta_0, \phi_0)}^{(3)}(3\pi/2) \rangle = \frac{1}{48} [15 + \cos(4\theta_0) + (1 + 3 \cos(2\theta_0)) \sin^4 \theta_0 \sin^2(2\phi_0)]. \quad (3)$$

This takes values in the narrow interval  $[7/24, 1/3]$ , and is shown in Fig. (1). The minimum corresponds to several initial states including  $|\pi/4, \pm\pi/2\rangle$  and the maximum includes the  $|0, 0\rangle$  and  $|\pi/2, \pm\pi/2\rangle$  states as already noted above. The structures seen are not directly linked to classical phase space orbits, except through shared symmetries [32], and cannot be expected to do so as the classical limit is for fixed  $\kappa_0$  and  $j \rightarrow \infty$ . Nevertheless these results lend quantitative credence to thermalization in the sense that the time averaged entropy of subsystems of most states are close to the ensemble average for suitable large  $\kappa_0$ , even for the 3-qubit case [7, 19].

The solution to the 3-qubit case proceeds from the general observation that  $[\mathcal{U}, \otimes_{l=1}^{2j} \sigma_l^y] = 0$ , *i.e.*, there

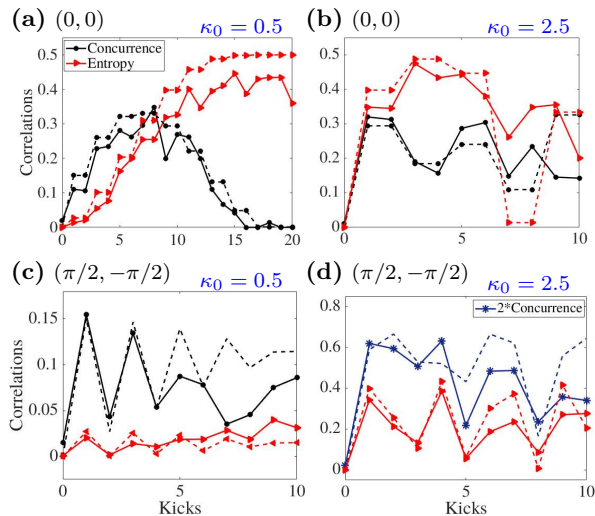


FIG. 2. Plots showing analytical (dashed curves with markers), experimental (solid curves with markers) and numerical (dashed) curves of linear entropy and concurrence as a function of the number of kicks, as the initial state  $|\psi_0\rangle$  is evolved under repeated applications of operator  $\mathcal{U}$ . Parameters of the initial state,  $(\theta_0, \phi_0)$ , and chaoticity parameter,  $\kappa_0$ , are specified in each figure. Analytical (wherever plotted) and numerical curves exactly overlap, and hence can not be seen separately.

is an “up-down” or parity symmetry. The standard 4-dimensional spin quartet permutation symmetric space with  $j = 3/2$ ,  $\{|000\rangle, |W\rangle = (|001\rangle + |010\rangle + |100\rangle)/\sqrt{3}, |\bar{W}\rangle = (|110\rangle + |101\rangle + |011\rangle)/\sqrt{3}, |111\rangle\}$  is parity symmetry adapted to form the basis

$$\left\{ |\phi_1^\pm\rangle = \frac{1}{\sqrt{2}}(|000\rangle \mp i|111\rangle), |\phi_2^\pm\rangle = \frac{1}{\sqrt{2}}(|W\rangle \pm i|\bar{W}\rangle) \right\}. \quad (4)$$

In this basis  $\mathcal{U}$  block diagonalizes into two  $2 \times 2$  blocks,

$$\mathcal{U}_\pm = \pm e^{\mp \frac{i\pi}{4}} e^{-i\kappa} \begin{pmatrix} \frac{i}{2} e^{-2i\kappa} & \mp \frac{\sqrt{3}}{2} e^{-2i\kappa} \\ \pm \frac{\sqrt{3}}{2} e^{2i\kappa} & -\frac{i}{2} e^{2i\kappa} \end{pmatrix}, \quad (5)$$

corresponding to parity eigenvalue  $\pm 1$ , spanned by  $\{|\phi_1^+\rangle, |\phi_2^+\rangle\}$ , and  $\{|\phi_1^-\rangle, |\phi_2^-\rangle\}$ . For simplicity the parameter  $\kappa = \kappa_0/6$  is used in these expressions. To evolve initial states we need  $\mathcal{U}^n$  and therefore  $\mathcal{U}_\pm^n$ . Expressing Eq. (5) as a rotation and a phase, enables the explicit formula [38]

$$\mathcal{U}_\pm^n = (\pm 1)^n e^{-in(\pm \frac{\pi}{4} + \kappa)} \begin{pmatrix} \alpha_n & \mp \beta_n^* \\ \pm \beta_n & \alpha_n^* \end{pmatrix}, \quad (6)$$

where  $\alpha_n = T_n(\chi) + \frac{i}{2} U_{n-1}(\chi) \cos 2\kappa$  and  $\beta_n = (\sqrt{3}/2) U_{n-1}(\chi) e^{2i\kappa}$ . The Chebyshev polynomials  $T_n(\chi)$  and  $U_{n-1}(\chi)$  are defined as  $T_n(\chi) = \cos(n\theta)$  and  $U_{n-1}(\chi) = \sin(n\theta)/\sin\theta$  with  $\chi = \cos\theta = \sin(2\kappa)/2$ .

It is straightforward to do time evolution now, for the state on the period-4 orbit, corresponding to the coherent

state at  $(0, 0)$  which is  $\otimes^3|0\rangle$ .

$$\mathcal{U}^n|000\rangle \equiv |\psi_n\rangle = \frac{1}{2} e^{-in(\frac{3\pi}{4} + \kappa)} \left\{ (1 + i^n)(\alpha_n|000\rangle + i\beta_n|\bar{W}\rangle) + (1 - i^n)(i\alpha_n|111\rangle - \beta_n|W\rangle) \right\}. \quad (7)$$

From the 1 and 2 qubit reduced density matrices  $\rho_1(n) = \text{tr}_{2,3}(|\psi_n\rangle\langle\psi_n|)$ ,  $\rho_{12}(n) = \text{tr}_3(|\psi_n\rangle\langle\psi_n|)$ , the entanglement of one qubit with the other two is measured by its entropy, and the entanglement between two qubits by the concurrence measure [39]. It turns out that for even values of the time  $n$ ,  $\rho_1(n)$  is diagonal and its eigenvalues are  $\lambda(n, \kappa) = \frac{1}{2} U_{n-1}^2(\chi)$  and  $1 - \lambda(n, \kappa)$ , from which the linear entropy  $S_{(0,0)}^{(3)}(n, \kappa) = 2\lambda(n, \kappa)(1 - \lambda(n, \kappa))$  and its infinite time average of Eq. (2) follows. The two-qubit state is an “X state” [40] when the time is even, and results in the concurrence being [38]

$$\mathcal{C}(n) = |U_{n-1}(\chi)| \left| \frac{1}{2} |U_{n-1}(\chi)| - \sqrt{1 - \frac{3}{4} |U_{n-1}(\chi)|^2} \right|. \quad (8)$$

Figure 2 shows the comparison between these analytical results and those using experimental data from [19], where two values of  $\kappa_0$ , 0.5 and 2.5 have been used. The experimental data is the result of full state tomography and the procedure we have used to analyze the data is outlined in the final section of the Supplementary materials [38]. The period-4 orbit is unstable at  $\kappa_0 = 2.5$  and we see a rapid growth in the entanglement. However even at  $\kappa_0 = 0.5$  entanglement grows to near maximal values, consistent with the large time average in Eq. (2) and Fig. (1). We need use only even values of the time as for this state,  $S(2n, \kappa) = S(2n - 1, \kappa)$  and results in the steps of the top panel in Fig. 2. This is exact in the analytical expressions and quite remarkably present (but previously unnoticed) in the experimental data for the first few time steps. This curiosity results from  $\mathcal{U}^{-1}|\psi_{2m}\rangle$  being locally equivalent to  $|\psi_{2m}\rangle$ . If  $m$  itself is even, then it is straightforward to verify that applying the non-local part of the unitary operator  $\mathcal{U}^{-1}$  results in  $\otimes^3 e^{i\kappa\sigma_z} |\psi_{2m}\rangle$ , hence  $|\psi_{2m-1}\rangle$  is locally connected to  $|\psi_{2m}\rangle$ , and all entanglement properties including concurrence is left unchanged for an odd-to-even time step. A similar situation holds when  $m$  is odd.

When the initial state is  $\otimes^3|+\rangle_y$  corresponding to the coherent state at  $(\pi/2, \pi/2)$ , the evolution lies entirely in the positive parity sector:  $\mathcal{U}^n|+++\rangle_y =$

$$\frac{1}{2} e^{-in(\frac{\pi}{4} + \kappa)} \left( (\alpha_n - i\sqrt{3}\beta_n^*) |\phi_1^+\rangle + (\beta_n + i\sqrt{3}\alpha_n^*) |\phi_2^+\rangle \right), \quad (9)$$

Eigenvalues of the corresponding  $\rho_1(n)$  are  $\lambda(n, \kappa) = 2\chi^2 U_{n-1}(\chi)^2$  and  $1 - \lambda(n, \kappa)$ , and the linear entropy is

$$S_{(\frac{\pi}{2}, \frac{\pi}{2})}^{(3)}(n, \kappa) = 4\chi^2 U_{n-1}(\chi)^2 (1 - 2\chi^2 U_{n-1}(\chi)^2). \quad (10)$$

See [38] for details. The plot showing comparison of linear entropy from experimental data and this expression

for  $\kappa_0 = 0.5$  and  $\kappa_0 = 2.5$  are shown in Fig. (2). It shows a much smaller growth for  $\kappa = 0.5$  in comparison to the state  $|000\rangle$ , reflecting the stable neighborhood of  $(\pi/2, \pi/2)$ . This being consistent with the long time average, already displayed in Eq. (2) which is derived from this expression. Qualitative discussions of the time-evolution have already been presented in [24] and we move on to the 4-qubit case.

*Exact solution for four-qubits:* In this case the parity symmetry reduced and permutation symmetric basis in which  $\mathcal{U}$  is block-diagonal is  $\{|\phi_1^\pm\rangle = \frac{1}{\sqrt{2}}(|W\rangle \mp |\overline{W}\rangle), |\phi_2^\pm\rangle = \frac{1}{\sqrt{2}}(|0000\rangle \pm |1111\rangle), |\phi_3^\pm\rangle = \frac{1}{\sqrt{6}}\sum_{\mathcal{P}}|0011\rangle_{\mathcal{P}}\}$ , where  $|W\rangle = \frac{1}{2}\sum_{\mathcal{P}}|0001\rangle_{\mathcal{P}}$ ,  $|\overline{W}\rangle = \frac{1}{2}\sum_{\mathcal{P}}|1110\rangle_{\mathcal{P}}$ , and  $\sum_{\mathcal{P}}$  sums over all possible permutations. A peculiarity of 4-qubits is that  $|\phi_1^\pm\rangle$  is an eigenstate of  $\mathcal{U}$  with eigenvalue  $-1$  for *all* values of the parameter  $\kappa_0$ . Thus the 5-dimensional space splits into  $1 \oplus 2 \oplus 2$  subspaces on which the operators are  $\mathcal{U}_0 = -1$  and  $\mathcal{U}_\pm$ .

The explicit form of powers of the  $2 \times 2$  blocks of  $\mathcal{U}$  are [38]

$$\mathcal{U}_+^n = e^{-\frac{in}{2}(\pi+\kappa)} \begin{pmatrix} \alpha_n & i\beta_n^* \\ i\beta_n & \alpha_n^* \end{pmatrix}, \text{ and} \quad (11)$$

$$\mathcal{U}_-^n = e^{-\frac{3i}{4}n\kappa} \begin{pmatrix} \cos \frac{n\pi}{2} & e^{\frac{3i}{4}\kappa} \sin \frac{n\pi}{2} \\ -e^{-\frac{3i}{4}\kappa} \sin \frac{n\pi}{2} & \cos \frac{n\pi}{2} \end{pmatrix} \quad (12)$$

where  $\alpha_n = T_n(\chi) + \frac{i}{2}U_{n-1}(\chi) \cos \kappa$ ,  $\beta_n = \frac{\sqrt{3}}{2}U_{n-1}(\chi)e^{i\kappa}$  and  $\chi = \frac{1}{2} \sin \kappa$ , with  $\kappa = \kappa_0/2$ . Using these it is possible to find the exact evolution of the entanglement entropy of any one-qubit and again in particular for the states  $|0000\rangle, |\pm \pm \pm \pm\rangle_y$  this gives their long-time averaged linear entropy (for  $\kappa_0 \neq 0, 2\pi$ ) as [38]

$$\langle S_{(0,0)}^{(4)}(\kappa_0) \rangle = \frac{1}{8} \left( \frac{9 + 2s_0}{3 + s_0} \right), \quad \langle S_{(\frac{\pi}{2}, \pm \frac{\pi}{2})}^{(4)}(\kappa_0) \rangle = \frac{1}{8} \left( \frac{9 - s_0}{3 + s_0} \right).$$

where  $s_0 = \cos^2(\kappa_0/2)$ . Both reach their maximum value of  $3/8$  when  $\kappa_0 = \pi$  and, remarkably, this matches with the average from the ensemble of random permutation symmetric states [37] of 4-qubits  $S_{RMT}(4)$  as in the case of the 3-qubit case. In addition we see that the average for the states at  $(\pi/2, \pm\pi/2)$  attain the value of  $1/4$  for arbitrarily small  $\kappa_0$  in contrast to the 3-qubit case which vanishes as in Eq. (2). In fact the non-zero average is seen in numerical calculations to be attained only on averaging over extremely long times for small  $\kappa_0$ .

This very slow process is due to tunneling between  $\otimes^4|+\rangle_y$  and  $\otimes^4|-\rangle_y$ . At  $\kappa_0 = 0$ , two positive parity eigenvectors of  $\mathcal{U}$ ,  $|\phi_1^+\rangle$  and  $|\phi_{23}^+\rangle = \frac{1}{2}|\phi_2^+\rangle - \frac{\sqrt{3}}{2}|\phi_3^+\rangle$  are degenerate with eigenvalue  $-1$ . These can also be written as 4-qubit GHZ states [41, 42]:  $i|\phi_1^+\rangle = (\otimes^4|+\rangle_y - \otimes^4|-\rangle_y)/\sqrt{2}$ , the unchanging eigenstate, and

$|\phi_{23}^+\rangle = (\otimes^4|+\rangle_y + \otimes^4|-\rangle_y)/\sqrt{2}$ . Thus

$$\mathcal{U}^n \otimes^4|+\rangle_y = (-1)^n \frac{i}{\sqrt{2}}|\phi_1^+\rangle + \mathcal{U}_+^n \frac{1}{\sqrt{2}}|\phi_{23}^+\rangle. \quad (13)$$

The eigenvalue of  $\mathcal{U}_+$  that is  $-1$  at  $\kappa_0 = 0$  is  $e^{i\gamma_-}$  with

$$\gamma_- = \frac{\kappa_0}{4} + \pi - \sin^{-1} \left( \frac{1}{2} \sin \frac{\kappa_0}{2} \right) \approx \pi - \frac{\kappa_0^3}{128}. \quad (14)$$

This implies that for  $\kappa_0 \ll 1$ , the corresponding state and  $|\phi_1^+\rangle$  are nearly degenerate. The splitting leads to a change in the relative phase of their contributions in Eq. (13) and at time  $n_* \approx 128\pi/\kappa_0^3$  the evolved state is close to  $\otimes^4|-\rangle_y$ , leading to tunneling as shown in Fig. (3) between what in the classical limit are two stable islands. At time  $n = n_*/2$  the state obtained is close to the GHZ state  $(\otimes^4|+\rangle_y - i\otimes^4|-\rangle_y)/\sqrt{2}$ .

This tunneling is observed whenever  $\otimes^{2j}|\pm\rangle$  are degenerate eigenstates of the rotation part of the Floquet  $\mathcal{U}$ . This implies that the number of qubits should be an integer multiple of  $2\pi/p$ , where  $p$  is the rotation angle (we have used  $p = \pi/2$ , and hence the tunneling occurs when the number of qubits is a multiple of 4).

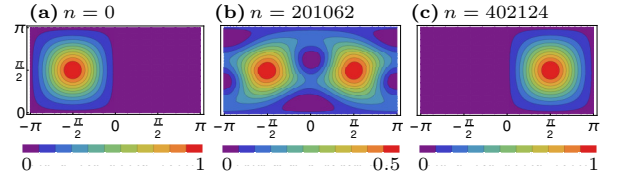


FIG. 3. Husimi (quasi probability distribution) plots for the four-qubit initial state,  $\otimes^4|+\rangle$ , evolving under  $n$  implementations of  $\mathcal{U}$ , and leading to tunneling to the state,  $\otimes^4|-\rangle$ , at time  $n_* \approx 128\pi/\kappa_0^3 \approx 402124$ . ( $\kappa_0 = 0.1$ ).

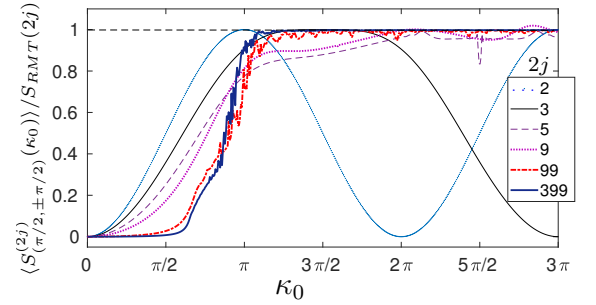


FIG. 4. Normalized average single-qubit entanglement when the initial state is  $\otimes^{2j}|+\rangle_y$  for increasing number of qubits (except multiples of 4 where there is tunneling for  $p = \pi/2$ .)

For larger number of qubits, the average single-qubit entropy, normalized by the random state average, is numerically found when the initial state is  $\otimes^{2j}|+\rangle_y$  and shown in Fig. (4). The trend is in keeping with a more complex classical phase space that becomes fully chaotic when the random state average is approached. The initial state being centered on a fixed point, increasing the

number of qubits leads to a sharp growth beyond  $\kappa_0 = 2$  when the fixed point becomes unstable, a more detailed study of this is found in [43]. Interestingly even for the 3-qubit case, for which we have the analytical evaluation in Eq. (2), a similar but smoother trend is displayed and reaches the random state value.

In summary, systems of few degrees of freedom, especially the exactly solvable 3- and 4- qubit instances of the kicked top provide insights into how entropy and entanglement thermalize in closed quantum systems in the sense of long time averages approaching ensemble averages. Experiments have already probed the 3-qubit case, which should be viewed as an integrable system. The 4-qubit case displays for the same rotation angle, tunneling and creation of GHZ states. Larger number of qubits can show genuine signatures of nonintegrability and chaos, and tunneling leads to creation of macroscopic superpositions that are generalized GHZ states. We hope our work raises new questions and adds to the discussion on the connections between integrability, quantum chaos, and thermalization.

We are grateful to the authors of [19] for generously sharing their experimental data, in particular to Pedram Roushan and Charles Neill for useful correspondence regarding the same.

- 
- [1] Patrick Billingsley. Prime numbers and brownian motion. *The American Mathematical Monthly*, 80(10):1099–1115, 1973.
- [2] M Kuś, R Scharf, and F Haake. Symmetry versus degree of level repulsion for kicked quantum systems. *Zeitschrift für Physik B Condensed Matter*, 66(1):129–134, 1987.
- [3] F. Haake. *Quantum Signatures of Chaos*. Springer-Verlag, Berlin, 1991.
- [4] Asher Peres. *Quantum Theory: Concepts and Methods*. Kluwer Academic Publishers, New York, 2002.
- [5] Amy C. Cassidy, Douglas Mason, Vanja Dunjko, and Maxim Olshanii. Threshold for chaos and thermalization in the one-dimensional mean-field bose-hubbard model. *Phys. Rev. Lett.*, 102:025302, Jan 2009.
- [6] Lea F. Santos and Marcos Rigol. Onset of quantum chaos in one-dimensional bosonic and fermionic systems and its relation to thermalization. *Phys. Rev. E*, 81:036206, Mar 2010.
- [7] Luca D’Alessio, Yariv Kafri, Anatoli Polkovnikov, and Marcos Rigol. From quantum chaos and eigenstate thermalization to statistical mechanics and thermodynamics. *Advances in Physics*, 65(3):239–362, 2016.
- [8] R. V. Jensen and R. Shankar. Statistical behavior in deterministic quantum systems with few degrees of freedom. *Phys. Rev. Lett.*, 54:1879–1882, Apr 1985.
- [9] J. M. Deutsch. Quantum statistical mechanics in a closed system. *Phys. Rev. A*, 43:2046–2049, 1991.
- [10] Mark Srednicki. Chaos and quantum thermalization. *Phys. Rev. E*, 50:888–901, 1994.
- [11] Marcos Rigol, Dunjko Vanja, and Olshanii Maxim. Thermalization and its mechanism for generic isolated quantum systems. *Nature*, 452(7189):854, 2009.
- [12] M. C. Bañuls, J. I. Cirac, and M. B. Hastings. Strong and weak thermalization of infinite nonintegrable quantum systems. *Phys. Rev. Lett.*, 106:050405, Feb 2011.
- [13] J. M. Deutsch, Haibin Li, and Auditya Sharma. Microscopic origin of thermodynamic entropy in isolated systems. *Phys. Rev. E*, 87:042135, Apr 2013.
- [14] T Langen, R Geiger, M Kuhnert, B Rauer, and J Schmiedmayer. Local emergence of thermal correlations in an isolated quantum many-body system. *Nature*, 9:640, 2013.
- [15] Luca D’Alessio and Marcos Rigol. Long-time behavior of isolated periodically driven interacting lattice systems. *Phys. Rev. X*, 4:041048, Dec 2014.
- [16] Achilleas Lazarides, Arnab Das, and Roderich Moessner. Periodic thermodynamics of isolated quantum systems. *Phys. Rev. Lett.*, 112:150401, Apr 2014.
- [17] Achilleas Lazarides, Arnab Das, and Roderich Moessner. Equilibrium states of generic quantum systems subject to periodic driving. *Phys. Rev. E*, 90:012110, Jul 2014.
- [18] Asmi Haldar, Roderich Moessner, and Arnab Das. Onset of floquet thermalization. *Phys. Rev. B*, 97:245122, Jun 2018.
- [19] C. Neill, P. Roushan, M. Fang, Y. Chen, M. Kolodrubetz, Z. Chen, A. Megrant, R. Barends, B. Campbell, B. Chiaro, A. Dunsworth, E. Jeffrey, J. Kelly, J. Mutus, P. J. J. OMalley, C. Quintana, D. Sank, A. Vainsencher, J. Wenner, T. C. White, A. Polkovnikov, and J. M. Martinis. Ergodic dynamics and thermalization in an isolated quantum system. *Nature Physics*, 12:1037, 2016.
- [20] Adam M. Kaufman, M. Eric Tai, Alexander Lukin, Matthew Rispoli, Robert Schittko, Philipp M. Preiss, and Markus Greiner. Quantum thermalization through entanglement in an isolated many-body system. *Science*, 353(6301):794–800, 2016.
- [21] Govinda Clos, Diego Porras, Ulrich Warring, and Tobias Schaetz. Time-resolved observation of thermalization in an isolated quantum system. *Phys. Rev. Lett.*, 117:170401, Oct 2016.
- [22] Kaden R. A. Hazzard, Mauritz van den Worm, Michael Foss-Feig, Salvatore R. Manmana, Emanuele G. Dalla Torre, Tilman Pfau, Michael Kastner, and Ana Maria Rey. Quantum correlations and entanglement in far-from-equilibrium spin systems. *Phys. Rev. A*, 90:063622, Dec 2014.
- [23] M. C. Gutzwiller. *Chaos in Classical and Quantum Mechanics*. Springer-Verlag, New York, 1990.
- [24] Vaibhav Madhok, Shruti Dogra, and Arul Lakshminarayan. Quantum correlations as probes of chaos and ergodicity. *Optics Communications*, 420:189 – 193, 2018.
- [25] Michael J. Davis and Eric J. Heller. Quantum dynamical tunneling in bound states. *The Journal of Chemical Physics*, 75(1):246–254, 1981.
- [26] W. A. Lin and L. E. Ballentine. Quantum tunneling and chaos in a driven anharmonic oscillator. *Phys. Rev. Lett.*, 65:2927–2930, Dec 1990.
- [27] Asher Peres. Dynamical quasidegeneracies and quantum tunneling. *Phys. Rev. Lett.*, 67:158–158, Jul 1991.
- [28] Steven Tomsovic, editor. *Tunneling in complex systems*. World Scientific, Singapore, 1998.
- [29] Srihari Keshavamurthy and Peter Schlagheck, editors. *Dynamical Tunneling Theory and Experiment*. CRC Press, Boca Raton, FL, 2011.
- [30] G. J. Milburn. Simulating nonlinear spin models in an

ion trap, 1999.

- [31] Xiaoguang Wang, Shohini Ghose, Barry C. Sanders, and Bambi Hu. Entanglement as a signature of quantum chaos. *Phys. Rev. E*, 70:016217, 2004.
- [32] Joshua B. Ruebeck, Jie Lin, and Arjendu K. Pattanayak. Entanglement and its relationship to classical dynamics. *Phys. Rev. E*, 95:062222, 2017.
- [33] Tomaž Prosen. Exact time-correlation functions of quantum ising chain in a kicking transversal magnetic field-spectral analysis of the adjoint propagator in heisenberg picture. *Progress of Theoretical Physics Supplement*, 139:191–203, 2000.
- [34] Arul Lakshminarayan and V. Subrahmanyam. Multipartite entanglement in a one-dimensional time-dependent ising model. *Phys. Rev. A*, 71:062334, Jun 2005.
- [35] Roy J. Glauber and Fritz Haake. Superradiant pulses and directed angular momentum states. *Phys. Rev. A*, 13:357, Oct 1976.
- [36] R. R. Puri. *Mathematical Methods of Quantum Optics*. Springer, Berlin, 2001.
- [37] A. Seshadri, V. Madhok, and A. Lakshminarayan. Tripartite mutual information, entanglement, and scrambling in permutation symmetric systems with an application to quantum chaos. *ArXiv e-prints*, May 2018.
- [38] See supplemental material at [url will be inserted by publisher] for further details.
- [39] William K. Wootters. Entanglement of formation of an arbitrary state of two qubits. *Phys. Rev. Lett.*, 80:2245–2248, 1998.
- [40] Ting Yu and J. H. Eberly. Evolution from entanglement to decoherence of bipartite mixed "x" states. *Quantum Info. Comput.*, 7(5):459–468, July 2007.
- [41] Daniel M. Greenberger, Michael A. Horne, and Anton Zeilinger. Going beyond bell's theorem. *arXiv:0712.0921 [quant-ph]*.
- [42] Daniel M. Greenberger, Michael A. Horne, Abner Shimony, and Anton Zeilinger. Bells theorem without inequalities. *American Journal of Physics*, 58(12):1131–1143, 1990.
- [43] Udaysinh T. Bhosale and M. S. Santhanam. Signatures of bifurcation on quantum correlations: Case of the quantum kicked top. *Phys. Rev. E*, 95:012216, Jan 2017.
- [44] Daniel F. V. James, Paul G. Kwiat, William J. Munro, and Andrew G. White. Measurement of qubits. *Phys. Rev. A*, 64:052312, 2001.
- [45] Matthias Steffen, M. Ansmann, Radoslaw C. Bialczak, N. Katz, Erik Lucero, R. McDermott, Matthew Neeley, E. M. Weig, A. N. Cleland, and John M. Martinis. Measurement of the entanglement of two superconducting qubits via state tomography. *Science*, 313(5792):1423–1425, 2006.
- [46] Erik Lucero, M. Hofheinz, M. Ansmann, Radoslaw C. Bialczak, N. Katz, Matthew Neeley, A. D. O'Connell, H. Wang, A. N. Cleland, and John M. Martinis. High-fidelity gates in a single josephson qubit. *Phys. Rev. Lett.*, 100:247001, 2008.

## SUPPLEMENTARY MATERIAL

In this section, we provide details of the results obtained in the main text of the manuscript and give further evidence of thermalisation. Last part of this supplementary material focuses on the analysis of the experimental data to obtain three-qubit density operators for various different initial states, after repeated implementations of the unitary operator  $\mathcal{U}$ .

### THREE-QUBIT SYSTEM UNDER A KICKED TOP HAMILTONIAN

This section contains a detailed description of the analytical solutions discussed in the main text file. As per Eq. (1) of the main text, unitary operator acting on a system of 3-qubits, that simulate the dynamics of a spin-3/2 under a kicked top Hamiltonian is given by,

$$\mathcal{U} = \exp\left(-i\frac{\kappa_0}{6}(\sigma_1^z\sigma_2^z + \sigma_2^z\sigma_3^z + \sigma_3^z\sigma_1^z)\right) \exp\left(-i\frac{\pi}{4}(\sigma_1^y + \sigma_2^y + \sigma_3^y)\right), \quad (15)$$

where  $\kappa_0$  is the chaoticity parameter and  $\sigma_i^{x,y,z}$  are the standard Pauli matrices. Since  $[\mathcal{U}, \sigma^y \otimes \sigma^y \otimes \sigma^y] = 0$ , we obtain eigenvectors of  $\sigma_{123}^y = \sigma^y \otimes \sigma^y \otimes \sigma^y$ , that block diagonalize  $\mathcal{U}$ . Eigenvectors of  $\sigma_{123}^y$  with eigenvalues  $\pm 1$  are given by

$$|\phi_1^\pm\rangle = \frac{1}{\sqrt{2}}(|000\rangle \mp i|111\rangle) \text{ and} \\ |\phi_2^\pm\rangle = \frac{1}{\sqrt{2}}(|W\rangle \pm i|\overline{W}\rangle), \quad (16)$$

where  $|\overline{W}\rangle = \frac{1}{\sqrt{3}}(|011\rangle + |101\rangle + |110\rangle)$ . Husimi plots for each of these bases vectors is shown in Fig.5. In this bases, the unitary operator ' $\mathcal{U}$ ' is written as

$$\mathcal{U} = \begin{pmatrix} \mathcal{U}_+ & 0_{2 \times 2} \\ 0_{2 \times 2} & \mathcal{U}_- \end{pmatrix}, \quad (17)$$

where  $0_{2 \times 2}$  is a null matrix, and  $2 \times 2$ -dimensional block  $\mathcal{U}_+$  ( $\mathcal{U}_-$ ) is written in the bases  $\{\phi_1^+, \phi_2^+\}$  ( $\{\phi_1^-, \phi_2^-\}$ ), thus being referred to as positive(negative)-parity subspace in our discussion. We have,

$$\mathcal{U}_\pm = \begin{pmatrix} \langle \phi_1^\pm | \mathcal{U} | \phi_1^\pm \rangle & \langle \phi_1^\pm | \mathcal{U} | \phi_2^\pm \rangle \\ \langle \phi_2^\pm | \mathcal{U} | \phi_1^\pm \rangle & \langle \phi_2^\pm | \mathcal{U} | \phi_2^\pm \rangle \end{pmatrix}. \quad (18)$$

This block diagonalization makes it easy to take the  $n^{\text{th}}$  power of the unitary operator  $\mathcal{U}$ ,

$$\mathcal{U}^n = \begin{pmatrix} \mathcal{U}_+^n & 0_{2 \times 2} \\ 0_{2 \times 2} & \mathcal{U}_-^n \end{pmatrix}. \quad (19)$$

The block operators  $\mathcal{U}_\pm$  are explicitly found by using Eqs.(15, 51, 18). We have,

$$\mathcal{U}_\pm = \pm e^{\mp \frac{i\pi}{4}} e^{-i\kappa} \begin{pmatrix} \frac{i}{2} e^{-2i\kappa} & \mp \frac{\sqrt{3}}{2} e^{-2i\kappa} \\ \pm \frac{\sqrt{3}}{2} e^{2i\kappa} & -\frac{i}{2} e^{2i\kappa} \end{pmatrix}, \quad (20)$$

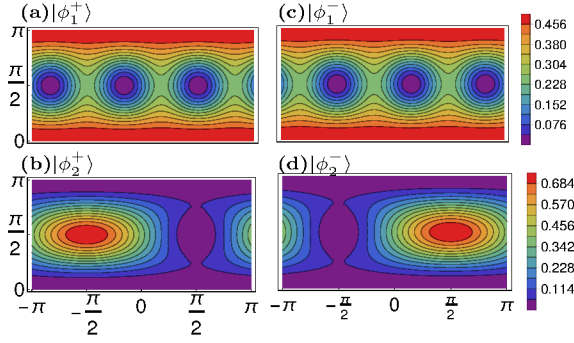


FIG. 5. Husimi (quasiprobability distribution,  $|\langle \phi_i | \theta_0, \phi_0 \rangle|^2$ ) plots for a set of four three-qubit bases states ( $|\phi_i\rangle$ ), where  $|\theta_0, \phi_0\rangle$  is an arbitrary three-qubit, parametrized by  $(\theta_0, \phi_0)$ .

For simplicity the parameter  $\kappa = \kappa_0/6$  is used in these expressions. One can easily flip between  $\mathcal{U}_+$  and  $\mathcal{U}_-$  using

$$\mathcal{U}_-(\kappa) = \mathcal{U}_+^*(-\kappa), \quad (21)$$

where  $*$  is the conjugation operation *in the standard bases*. Re-writing  $\mathcal{U}^\pm$  as a rotation by angle ' $\theta$ ' about an arbitrary axis ( $\hat{\eta} = \sin \alpha \cos \beta \hat{x} + \sin \alpha \sin \beta \hat{y} + \cos \alpha \hat{z}$ ),

$$\mathcal{U}_\pm \doteq e^{-i\theta \sigma^\eta} = \exp[-i\theta(\sin \alpha \cos \beta \sigma^x + \sin \alpha \sin \beta \sigma^y + \cos \alpha \sigma^z)], \quad (22)$$

which is valid upto phases. On comparison with Eq. 20, we obtain,  $\cos \theta = \frac{1}{2} \sin 2\kappa$ ,  $\beta = \pi/2 + 2\kappa$ , and  $\sin \alpha = \sqrt{3}/(2 \sin \theta)$ . To evolve initial states we need  $\mathcal{U}^n$  and therefore  $\mathcal{U}_\pm^n$ ,

$$\mathcal{U}_\pm^n = e^{-i\frac{n\pi}{4}} e^{-in\kappa} \begin{pmatrix} \cos n\theta - i \sin n\theta \cos \alpha & -i \sin n\theta \sin \alpha e^{-i\beta} \\ -i \sin n\theta \sin \alpha e^{i\beta} & \cos n\theta + i \sin n\theta \cos \alpha \end{pmatrix}. \quad (23)$$

Further,  $\cos(n\theta)$  and  $\sin(n\theta)/\sin \theta$  are identified as the Chebyshev polynomials of first kind ( $T_n(\chi)$ ) and second kind ( $U_{n-1}(\chi)$ ) respectively with  $\chi = \cos \theta = \sin(2\kappa)/2$ . Re-writing  $\mathcal{U}_\pm^n$  in a more convenient form,

$$\mathcal{U}_\pm^n = (\pm 1)^n e^{-in(\pm\frac{\pi}{4} + \kappa)} \begin{pmatrix} \alpha_n & \mp \beta_n^* \\ \pm \beta_n & \alpha_n^* \end{pmatrix}, \quad (24)$$

where  $\alpha_n = T_n(\chi) + \frac{i}{2} U_{n-1}(\chi) \cos 2\kappa$  and  $\beta_n = (\sqrt{3}/2) U_{n-1}(\chi) e^{2i\kappa}$ .

### Special case 1: $|\psi_0\rangle = |000\rangle$

Considering a three-qubit state  $|\psi_0\rangle = |000\rangle$ , under the action of  $n$  implementations of  $U$ ,

$$\begin{aligned} \mathcal{U}^n |000\rangle &= \frac{1}{\sqrt{2}} \mathcal{U}^n (|\phi_1^+\rangle + |\phi_1^-\rangle) \\ &= \frac{1}{\sqrt{2}} (\mathcal{U}_+^n |\phi_1^+\rangle + \mathcal{U}_-^n |\phi_1^-\rangle). \end{aligned} \quad (25)$$

Final state of three-qubit system ( $|\psi_n\rangle$ ), after  $n$  implementations of the unitary operator  $\mathcal{U}$  on  $|\psi_0\rangle$ , is given by (from Eq.(24)),

$$\begin{aligned} \mathcal{U}^n |000\rangle \equiv |\psi_n\rangle &= \frac{1}{2} e^{-in(\frac{3\pi}{4} + \kappa)} \{ (1 + i^n) (\alpha_n |000\rangle \\ &+ i \beta_n |\overline{W}\rangle) + (1 - i^n) (i \alpha_n |111\rangle - \beta_n |W\rangle) \}. \end{aligned} \quad (26)$$

We further study correlations such as linear entropy of the single-qubit reduced state ( $\rho_1$ ) of  $\rho_n = |\psi_n\rangle\langle\psi_n|$  and concurrence ( $\mathcal{C}$ ) between any two qubits,

### Linear entropy (for even values of 'n')

Single-party reduced density operator is obtained by tracing out any of the two qubits of the three-qubit density operator,

$$\rho_1 = \text{Tr}_{2,3} |\psi_n\rangle\langle\psi_n|$$

For even values of 'n', eigenvalues of the single qubit state are,  $\lambda_n^{(1)} = \lambda_n$  and  $\lambda_n^{(2)} = 1 - \lambda_n$ , where  $\lambda_n = \frac{2}{3} |\beta_n|^2$ . Therefore the measure of entanglement based on linear entropy,

$$S_{(0,0)}^{(3)}(n, \kappa) = 1 - \sum_{i=1}^2 (\lambda_n^{(i)})^2 = 2(\lambda_n)(1 - \lambda_n), \quad (27)$$

where,  $\lambda_n = \frac{1}{2} U_{n-1}^2(\chi)$ . It is also interesting to look at long-time averaged linear entropy. Re-writing Eq. 27 as,

$$\begin{aligned} S_{(0,0)}^{(3)}(n, \kappa) &= U_{n-1}^2(\chi) - \frac{1}{2} U_{n-1}^4(\chi) \\ &= \frac{\sin^2 n\theta}{\sin^2 \theta} - \frac{1}{2} \frac{\sin^4 n\theta}{\sin^4 \theta}, \end{aligned} \quad (28) \quad (29)$$

Long-time averaged linear entropy,

$$\begin{aligned} \langle S_{(0,0)}^{(3)}(\kappa) \rangle &= \frac{1}{\sin^2 \theta} \langle \sin^2 n\theta \rangle - \frac{1}{2 \sin^4 \theta} \langle \sin^4 n\theta \rangle, \\ &= \frac{1}{2 \sin^2 \theta} - \frac{3}{16 \sin^4 \theta}. \end{aligned} \quad (30) \quad (31)$$

Further, using  $\cos \theta = \frac{1}{2} \sin 2\kappa$ , we obtain,

$$\langle S_{(0,0)}^{(3)}(\kappa) \rangle = \frac{5 - 2 \sin^2(2\kappa)}{(4 - \sin^2(2\kappa))^2}, \quad (32)$$

that attains its maximum value of  $1/3$  at  $\kappa = \pi/4$ .

### Concurrence (for even values of 'n')

$$\rho_{12} = \begin{pmatrix} |\alpha_n|^2 & 0 & 0 & -\frac{i}{\sqrt{3}} \alpha_n \beta_n^* \\ 0 & \frac{1}{3} |\beta_n|^2 & \frac{1}{3} |\beta_n|^2 & 0 \\ 0 & \frac{1}{3} |\beta_n|^2 & \frac{1}{3} |\beta_n|^2 & 0 \\ \frac{i}{\sqrt{3}} \alpha_n^* \beta_n & 0 & 0 & \frac{1}{3} |\beta_n|^2 \end{pmatrix}, \quad (33)$$

which is an ‘ $X$ ’ state, whose concurrence,  $\mathcal{C}(\rho_{12})$  is measured by [40],  $2.\max\left[0, \frac{1}{3}|\beta_n|^2 - \frac{1}{\sqrt{3}}|\alpha_n||\beta_n|, -(\frac{1}{3}|\beta_n|^2 - \frac{1}{\sqrt{3}}|\alpha_n||\beta_n|)\right]$ . Thus,

$$\mathcal{C}(\rho_{12}) = 2 \left| \frac{1}{3}|\beta_n|^2 - \frac{1}{\sqrt{3}}|\alpha_n||\beta_n| \right|. \quad (34)$$

Substituting the values of  $\alpha_n$  and  $\beta_n$ , concurrence is given by

$$\mathcal{C}(\rho_{12}) = |U_{n-1}(\chi)| \left| \frac{1}{2}|U_{n-1}(\chi)| - \sqrt{1 - \frac{3}{4}|U_{n-1}(\chi)|^2} \right|. \quad (35)$$

#### Correlations for odd values of ‘ $n$ ’

To obtain the values of linear entropy and concurrence for states (in Eq.(26)) for odd values of  $n$ , one can evolve the even  $n = 2m$  states one step backward or forward in time, such as,

$$|\phi_{2m-1}\rangle = \mathcal{U}^{-1}|\phi_{2m}\rangle, \quad (36)$$

where  $\mathcal{U}$  is the unitary operator (given in Eq.15). Considering the backward evolution of  $|\phi_{2m}\rangle$  (say for even value of  $m$ ), under the non-local part of the unitary operator  $\mathcal{U}$ ,

$$\begin{aligned} |\psi_{2m-1}\rangle &= e^{i\kappa(\sigma_1^z \sigma_2^z + \sigma_2^z \sigma_3^z + \sigma_3^z \sigma_1^z)} (\alpha_{2m}|000\rangle + i\beta_{2m}|\overline{W}\rangle), \\ &= e^{3i\kappa} \alpha_{2m}|000\rangle + ie^{-i\kappa} \beta_{2m}|\overline{W}\rangle, \\ &= \mathcal{V} \otimes \mathcal{V} \otimes \mathcal{V} |\phi_{2m}\rangle, \end{aligned} \quad (37)$$

where single qubit unitary operator  $\mathcal{V} = e^{i\kappa\sigma_z}$ . Thus the three qubit state  $|\psi_0\rangle$ , after odd numbered implementations of the unitary operator  $\mathcal{U}$  are locally connected to the state obtained after even numbered implementations of the operator  $\mathcal{U}$ .

#### Special case 2: $|\psi_0\rangle = |+++ \rangle$

Considering a three-qubit state,  $|\psi_0\rangle = |+++ \rangle$ , where  $|+\rangle = \frac{1}{\sqrt{2}}(|0\rangle + i|1\rangle)$  is an eigenvector of  $\sigma_y$  with eigenvalue  $+1$ . Three qubit state is explicitly written as

$$|\psi_0\rangle = \frac{1}{2} \left( |\phi_1^+\rangle + i\sqrt{3}|\phi_2^+\rangle \right), \quad (38)$$

which lies in the positive parity subspace. Three qubit state after  $n$  implementations of  $\mathcal{U}$  is given by (upto an overall phase),

$$|\psi_n\rangle = \frac{1}{2} e^{-in(\frac{\pi}{4} + \kappa)} (\gamma_n |\phi_1^+\rangle + \delta_n |\phi_2^+\rangle), \quad (39)$$

where  $\gamma_n = \alpha_n - i\sqrt{3}\beta_n^*$  and  $\delta_n = \beta_n + i\sqrt{3}\alpha_n^*$ . One can obtain the single-party reduced state by tracing out any two-qubits,

$$\rho_A = \frac{1}{4} \begin{pmatrix} \frac{1}{2} (|\gamma_n|^2 + |\delta_n|^2) & -\frac{i}{3} (|\delta_n|^2 - \sqrt{3} \text{Im}(\gamma_n \delta_n^*)) \\ \frac{i}{3} (|\delta_n|^2 - \sqrt{3} \text{Im}(\gamma_n \delta_n^*)) & \frac{1}{2} (|\gamma_n|^2 + |\delta_n|^2) \end{pmatrix}. \quad (40)$$

Eigenvalues of  $\rho_A$  are  $\frac{1}{2} \pm |\rho_A(1, 2)|$ , which are explicitly given by

$$\lambda_n^{(1)} = 2\chi^2 U_{n-1}(\chi)^2 \text{ and } \lambda_n^{(2)} = 1 - 2\chi^2 U_{n-1}(\chi)^2. \quad (41)$$

Linear entropy of this single-party reduced state is found to be

$$S_{(\frac{\pi}{2}, -\frac{\pi}{2})}^{(3)}(n, \kappa) = \frac{1}{2} - 2|\rho_A(1, 2)|^2 = 2\lambda_n(1 - \lambda_n), \quad (42)$$

which in a much simplified form is given by

$$S_{(\frac{\pi}{2}, -\frac{\pi}{2})}^{(3)}(n, \kappa) = 4\chi^2 U_{n-1}(\chi)^2 (1 - 2\chi^2 U_{n-1}(\chi)^2). \quad (43)$$

We also obtain the long time-average value of the linear entropy, given by,

$$\langle S_{(\frac{\pi}{2}, -\frac{\pi}{2})}^{(3)}(\kappa) \rangle = \frac{\sin^2(2\kappa)}{(4 - \sin^2(2\kappa))^2} (8 - 5\sin^2(2\kappa)), \quad (44)$$

which, when  $\kappa = \pi/4$  approaches  $1/3$ . Coincidentally, this is same as the average linear entropy of a single-qubit reduced state in a set of random symmetric three-qubit states.

#### Linear entropy of an arbitrary three-qubit permutation symmetric state

Considering a three-qubit state

$$|\psi_0\rangle = a_1|\phi_1^+\rangle + a_2|\phi_2^+\rangle + b_1|\phi_1^-\rangle + b_2|\phi_2^-\rangle. \quad (45)$$

Each of the three qubits are initialized in the same state ( $|\psi\rangle = \cos\frac{\theta_0}{2}|0\rangle + e^{-i\phi_0}\sin\frac{\theta_0}{2}|1\rangle$ , in the computational bases), such that the initial state of the 3-qubit system is  $|\psi_0\rangle = \otimes^3|\psi\rangle$ , where  $\theta_0 \in [0, \pi]$  and  $\phi_0 \in [-\pi, \pi]$ . Repeated implementations of the unitary operator  $\mathcal{U}$ , leads to  $|\psi_n\rangle = \mathcal{U}^n|\psi_0\rangle$ . We obtain single-party reduced density operator by tracing out any of the two qubits of the three-qubit density operator ( $\rho_n = |\psi_n\rangle\langle\psi_n|$ ), leading to,

$$\rho_i = \begin{pmatrix} r & s \\ s^* & 1 - r \end{pmatrix}, \quad (46)$$

where the elements of the density operator are given by

$$\begin{aligned} r &= \frac{1}{2} + \text{Re} \left( a_{1n} b_{1n}^* + \frac{1}{3} a_{2n} b_{2n}^* \right) \quad \text{and} \\ s &= \frac{1}{\sqrt{3}} \text{Re} (a_{1n} b_{2n}^* + b_{1n} a_{2n}^*) + \frac{i}{\sqrt{3}} \text{Im} (a_{1n} a_{2n}^* + b_{1n} b_{2n}^*) \\ &\quad - \frac{i}{3} (a_{2n} + b_{2n}) (a_{2n}^* - b_{2n}^*). \end{aligned} \quad (47)$$

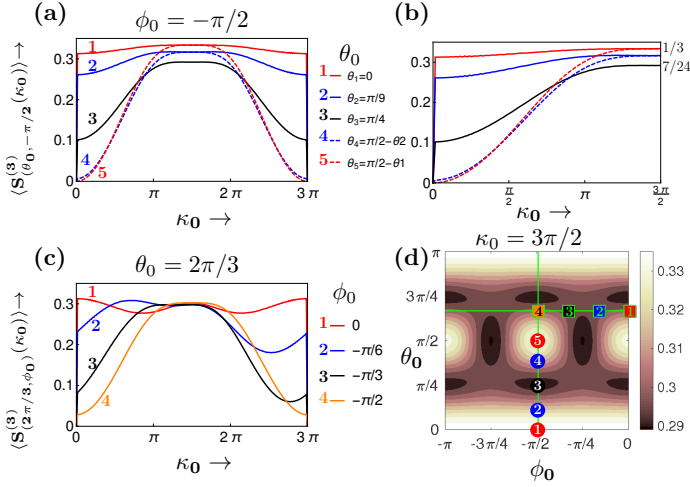


FIG. 6. (a),(b) Time averaged linear entropy ( $\langle S_{(\theta_0, -\pi/2)}^{(3)} \rangle$ ) of a single party reduced state vs chaoticity parameter  $\kappa_0$ . Different curves correspond to different initial states,  $|\theta_0, -\pi/2\rangle$  as labelled 1 to 5, alongwith explicit values of  $\theta_0$  given in the plot legends. These corresponding initial states  $|\theta_0, \phi_0\rangle$  are also marked as numbered circles in the contour plot given in part (d). Part (c) contains the plots for  $\langle S_{(2\pi/3, \phi_0)}^{(3)} \rangle$  vs chaoticity parameter  $\kappa_0$  for a fixed value of  $\theta_0 = 2\pi/3$ . Different curves correspond to different initial states, labelled by numbers 1 to 4 alongwith explicit values of  $\phi_0$  given in the plot legends. Respective initial states  $|\theta_0, \phi_0\rangle$  are also marked as numbered squares (with a green border) in the contour plot given in part (d). Contour plot shown in part (d) corresponds to  $\kappa_0 = 3\pi/2$ .

Where the coefficients,  $a_{1n} = a_1\alpha_n - a_2\beta_n^*$ ,  $a_{2n} = a_1\beta_n + a_2\alpha_n^*$ ,  $b_{1n} = i^n(b_1\alpha_n + b_2\beta_n^*)$ , and  $b_{2n} = i^n(b_2\alpha_n^* - b_1\beta_n)$ . Linear entropy of the single-qubit (Eq.(46)) is thus given by,

$$S_{(\theta_0, \phi_0)}^{(3)}(n, \kappa) = 2[r(1-r) - |s|^2]. \quad (48)$$

Thus linear entropy is obtained as a function of the initial-state parameters  $(\theta_0, \phi_0)$ . Long time average linear entropy is calculated numerically with  $n = 1000$  for various initial states as shown in Fig 6. Part (a) and (c) of Fig. 6 show the variation of time average entropy with chaoticity parameter for a period  $2\pi j$ . Pairs of complimentary  $\theta_0$ s, saturate to same values in the region around  $\kappa_0 = 3\pi/2$ . Part (b) of Fig 6 highlights the range of values of average linear entropy at  $\kappa_0 = 3\pi/2$ , a scale of similar range in part (d) depicts that the linear entropy of a single-qubit reduced state for an arbitrary value of parameters  $(\theta_0, \phi_0)$  fall into this range.

Further, we have obtained an explicit closed form expression for long time average linear entropy for an arbitrary  $(\theta_0, \phi_0)$  at  $\kappa_0 = 3\pi/2$ , which is discussed in the main text.

## FOUR QUBIT KICKED TOP

Considering a spin-2 system, whose dynamics is effectively simulated by a four-qubit system, confined to its five-dimensional symmetric subspace. Re-writing Eq. (1) from the main text, explicitly for a system of four qubits,

$$\mathcal{U} = \exp\left(-i\frac{\kappa_0}{8}(\sigma_1^z\sigma_2^z + \sigma_1^z\sigma_3^z + \sigma_1^z\sigma_4^z + \sigma_2^z\sigma_3^z + \sigma_2^z\sigma_4^z + \sigma_3^z\sigma_4^z)\right) \exp\left(-i\frac{\pi}{4}(\sigma_1^y + \sigma_2^y + \sigma_3^y + \sigma_4^y)\right), \quad (49)$$

where all the terms have their usual meanings. We have,

$$[\mathcal{U}, \sigma^y \otimes \sigma^y \otimes \sigma^y \otimes \sigma^y] = 0. \quad (50)$$

Unitary operator  $\mathcal{U}$  becomes block diagonal in the eigenbases of operator  $\sigma_{1234}^y = \otimes^4 \sigma^y$ , given by,

$$\begin{aligned} |\phi_1^\pm\rangle &= \frac{1}{\sqrt{2}}(|W\rangle \mp |\bar{W}\rangle) \\ &= \frac{1}{\sqrt{2}}\left(\frac{1}{2}\sum_{\mathcal{P}}|0001\rangle_{\mathcal{P}} \mp \frac{1}{2}\sum_{\mathcal{P}}|0111\rangle_{\mathcal{P}}\right), \\ |\phi_2^\pm\rangle &= \frac{1}{\sqrt{2}}(|0000\rangle \pm |1111\rangle), \text{ and} \\ |\phi_3^+\rangle &= \frac{1}{\sqrt{6}}\sum_{\mathcal{P}}|0011\rangle_{\mathcal{P}}, \end{aligned} \quad (51)$$

where  $\sum_{\mathcal{P}}$  sums over all possible permutations. Eigenvectors of  $\otimes^4 \sigma^y$ ,  $|\phi_i^+\rangle$  with eigenvalues  $+1$ , lie in the positive parity subspace, while  $|\phi_i^-\rangle$  with eigenvalues  $-1$  belong to the negative-parity subspace. Husimi plots for each of these bases vectors is shown in Fig.7. It is interesting to note that  $|\phi_1^+\rangle$  is also an eigenvector of  $\mathcal{U}_+$  with eigenvalue  $-1$ . In this set of bases, the unitary operator  $\mathcal{U}$  becomes block diagonal, which makes it easy to take the  $n^{\text{th}}$  power of the unitary operator  $\mathcal{U}$ ,

$$\mathcal{U}^n = \begin{pmatrix} \mathcal{U}_0^n & 0_{1\times 2} & 0_{1\times 2} \\ 0_{2\times 1} & \mathcal{U}_+^n & 0_{2\times 2} \\ 0_{2\times 1} & 0_{2\times 2} & \mathcal{U}_-^n \end{pmatrix}, \quad (52)$$

This simplifies our problem to much extent, which is now decomposed to work only in the  $2 \times 2$ -dimensional subspaces.

Various blocks are written here explicitly, we have

$$\mathcal{U}_0 = \langle \phi_1^+ | \mathcal{U} | \phi_1^+ \rangle = -1, \quad (53)$$

which is a part of the positive-parity subspace. Block  $\mathcal{U}_+$  is written in the bases  $\{\phi_2^+, \phi_3^+\}$ ,

$$\mathcal{U}_+ = -ie^{-\frac{i\kappa}{2}} \begin{pmatrix} \frac{i}{2}e^{-i\kappa} & \frac{\sqrt{3}i}{2}e^{-i\kappa} \\ \frac{\sqrt{3}i}{2}e^{i\kappa} & -\frac{i}{2}e^{i\kappa} \end{pmatrix}. \quad (54)$$

Block  $\mathcal{U}_-$  is written in the bases  $\{\phi_1^-, \phi_2^-\}$ ,

$$\mathcal{U}_- = e^{-\frac{3i\kappa}{4}} \begin{pmatrix} 0 & e^{\frac{3i\kappa}{4}} \\ -e^{-\frac{3i\kappa}{4}} & 0 \end{pmatrix} \quad (55)$$

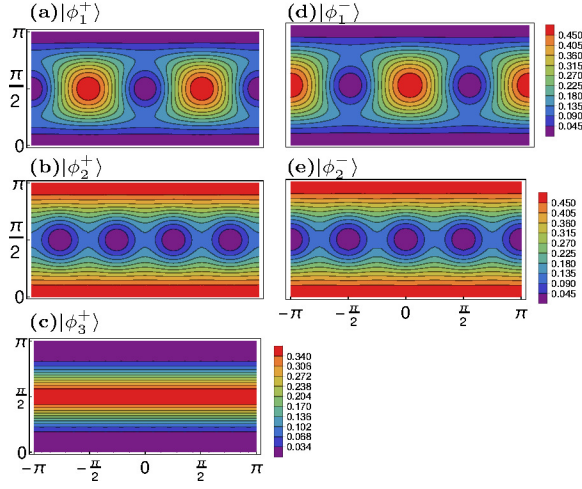


FIG. 7. Husimi (quasiprobability distribution,  $|\langle \phi_i | \theta_0, \phi_0 \rangle|^2$ ) plots for a set of five four-qubit bases states ( $|\phi_i\rangle$ ), where  $|\theta_0, \phi_0\rangle$  is an arbitrary four-qubit, parametrized by  $(\theta_0, \phi_0)$ .

Re-writing as a rotation ( $e^{i\theta\sigma^{\hat{\eta}}}$ ) by angle ‘ $\theta$ ’ about an arbitrary axis ( $\hat{\eta} = \sin \alpha \cos \beta \hat{x} + \sin \alpha \sin \beta \hat{y} + \cos \alpha \hat{z}$ ). The generator of this rotation being,  $\sigma^{\hat{\eta}} = \sin \alpha \cos \beta \sigma^x + \sin \alpha \sin \beta \sigma^y + \cos \alpha \sigma^z$ . A general rotation operator, raised to power ‘ $n$ ’ is thus of the form  $e^{in\theta\sigma^{\hat{\eta}}}$ . We have,

$$\begin{aligned} \mathcal{U}_+^n &= e^{-\frac{in(\pi+\kappa)}{2}} e^{in\theta\sigma^{\hat{\eta}}} \\ &= e^{-\frac{in(\pi+\kappa)}{2}} \begin{pmatrix} \cos n\theta + \frac{i \sin n\theta}{2} \cos \kappa & \frac{i\sqrt{3} \sin n\theta}{2} e^{-i\kappa} \\ \frac{i\sqrt{3} \sin n\theta}{2} e^{i\kappa} & \cos n\theta - \frac{i \sin n\theta}{2} \cos \kappa \end{pmatrix}, \end{aligned}$$

where  $\cos \theta = \sin \kappa/2$ ,  $\beta = \kappa$ ,  $\sin \alpha = \sqrt{3}/(2 \sin \theta)$ , and  $\cos \alpha = \cos \kappa/(2 \sin \theta)$ . Further simplification leads to the form,

$$\mathcal{U}_+^n = e^{-\frac{in(\pi+\kappa)}{2}} \begin{pmatrix} \alpha_n & i\beta_n^* \\ i\beta_n & \alpha_n^* \end{pmatrix}, \quad (56)$$

such that,

$$\begin{aligned} \alpha_n &= T_n(\chi) + \frac{i}{2} U_{n-1}(\chi) \cos \kappa \quad \text{and} \\ \beta_n &= \frac{\sqrt{3}}{2} U_{n-1}(\chi) e^{i\kappa}, \end{aligned} \quad (57)$$

where  $T_n(\chi)$  and  $U_{n-1}(\chi)$  are the Chebyshev polynomials of first and second kinds respectively, with  $\chi = \sin \kappa/2$ .

Further, comparing  $\mathcal{U}_3$  with the general rotation operator, we obtain,  $\theta = \pi/2, \alpha = \pi/2, \beta = -(\frac{\pi}{2} + \frac{3\kappa}{4})$ . Thus,

$$\mathcal{U}_-^n = e^{-\frac{3in\kappa}{4}} \begin{pmatrix} \cos \frac{n\pi}{2} & e^{\frac{3i\kappa}{4}} \sin \frac{n\pi}{2} \\ -e^{-\frac{3i\kappa}{4}} \sin \frac{n\pi}{2} & \cos \frac{n\pi}{2} \end{pmatrix} \quad (58)$$

**Special case 1:**  $|\psi_0\rangle = |0000\rangle$

Considering four qubit state  $|0000\rangle$ , under the ‘ $n$ ’ implementations of unitary operator  $\mathcal{U}$ ,

$$\mathcal{U}^n |0000\rangle = \frac{1}{\sqrt{2}} (\mathcal{U}_+^n |\phi_2^+\rangle + \mathcal{U}_-^n |\phi_2^-\rangle),$$

leading to final state  $|\psi_n\rangle$ . We further analyse single-qubit reduced density operator ( $\rho_1$ ) of the final state ( $\rho_n = |\psi_n\rangle\langle\psi_n|$ ) by tracing out any three qubits of the four qubit system. Single-qubit reduced density operator obtained in this case is diagonal for even values of  $n$ , eigenvalues being  $\lambda$  and  $1 - \lambda$ , where  $\lambda = \frac{1}{2} (1 + \text{Re}(\alpha_n e^{in\kappa_0/4}))$ . For even values of  $n$ , linear entropy of a single-qubit reduced state is given by,

$$S_{(0,0)}^{(4)}(n, \kappa_0) = \frac{1}{2} \left[ 1 - \left( \text{Re}(\alpha_n e^{in\kappa_0/4}) \right)^2 \right]. \quad (59)$$

Long time average of the linear entropy is obtained by averaging over  $n$  as shown in Section . Final expression for  $\langle S_{(0,0)}^{(4)} \rangle$  thus obtained, is discussed in the main text.

**Special case 2:**  $|\psi_0\rangle = |++++\rangle$

This state lies entirely in the positive parity subspace of our five dimensional permutation symmetric space of four qubits, given by

$$\otimes^4 |+\rangle = \frac{i}{\sqrt{2}} |\phi_1^+\rangle - \frac{1}{\sqrt{8}} |\phi_2^+\rangle + \sqrt{\frac{3}{8}} |\phi_3^+\rangle, \quad (60)$$

which under the action of  $\mathcal{U}^n$ , leads to  $|\psi_n\rangle = \mathcal{U}_+^n |++++\rangle$ . Reduced density operator of each of these four qubits is given by,

$$\rho_1 = \text{Tr}_{2,3,4} (|\psi_n\rangle\langle\psi_n|) = \begin{pmatrix} r_{(4)} & s_{(4)} \\ s_{(4)}^* & 1 - r_{(4)} \end{pmatrix}, \quad (61)$$

where, diagonal element,  $r_{(4)} = 1/2$  and  $s_{(4)} = \frac{i(-1)^n}{2} (\sin(\delta) U_{n-1}(\chi) \cos(\kappa_0/2) - T_n(\chi) \cos(\delta))$  with  $\delta = -n(2\pi + \kappa_0)/4$ . A closed form expression for long time average linear entropy is then obtained using,

$$S_{(\pi/2, -\pi/2)}^{(4)} = 2 \left( \langle r_{(4)} \rangle - \langle r_{(4)}^2 \rangle - \langle |s_{(4)}|^2 \rangle \right),$$

which is discussed in the main text.

## EXPERIMENTAL STATE RECONSTRUCTION

We analyse the data from a recent experiment [19], that demonstrates the kicked top dynamics of a spin-3/2, using three superconducting transmon qubits. State of a three-qubit system is obtained via complete quantum

state tomography using a set of 64 projective measurements. These projective measurements are constructed by taking the combinations of Pauli- $x, y, z$  matrices ( $\sigma_x, \sigma_y, \sigma_z$ ) and the Identity operator ( $I$ ) [19, 44]. These measurements are experimentally realized by various single-qubit rotations ( $\mathcal{R}$ ) followed by  $\sigma_z$  measurements on individual qubits, that effectively performs a  $\sigma'_i$  measurement (for  $i' = x, \mathcal{R} = \text{Hadamard operator } (Hd)$ ;  $i' = y, \mathcal{R} = \text{Phase shift } (\mathcal{S}).Hd$ ;  $i' = z, \mathcal{R} = I$ ) [19]. Multiple implementations of each measurement, provides the relative occupancy of the eight bases states of a three-qubit system. The resulting relative populations ( $p_m$ ) of the eight bases states are thus obtained experimentally. In order to compensate the effect of errors induced by the measurements, the intrinsic populations ( $p_{int}$ ) are obtained via a correction matrix ( $F$ ) [45, 46]. We have,  $p_{int} = F^{-1}p_m$ , where  $F = F_1 \otimes F_2 \otimes F_3$ .  $F_i$  is the measurement error corresponding to  $i^{th}$  qubit, given as,

$$F_i = \begin{pmatrix} f_0^{(i)} & 1 - f_1^{(i)} \\ 1 - f_0^{(i)} & f_1^{(i)} \end{pmatrix}.$$

Here,  $f_0^{(i)}$  is the probability by which a state  $|0\rangle$  of the  $i^{th}$  qubit is correctly identified as  $|0\rangle$ , while  $1 - f_1^{(i)}$  is

the probability by which, a state that is actually  $|0\rangle$  is being wrongly considered as  $|1\rangle$ .  $f_0^{(i)}$  and  $f_1^{(i)}$  are termed as the measurement fidelities of the bases states  $|0\rangle$  and  $|1\rangle$  respectively of the  $i^{th}$  qubit. Using part of the measurement data corresponding to the initial state preparation, we obtain the measurement fidelities:  $f_0^{(1)} = 0.98, f_1^{(1)} = 0.92, f_0^{(2)} = 0.98, f_1^{(2)} = 0.94, f_0^{(3)} = 0.96, f_1^{(3)} = 0.87$ . The intrinsic populations obtained in this manner are positive (as observed till second decimal place). Using these intrinsic population values, three-qubit density operators are obtained, that further undergo the convex optimization. The fidelities between the theoretically expected ( $\rho_t$ ) and the experimentally obtained ( $\rho_e$ ) states is given by [19]

$$\mathcal{F} = Tr \sqrt{\sqrt{\rho_t} \rho_e \sqrt{\rho_t}}. \quad (62)$$

These experimentally obtained three-qubit density operators are then used in our study to obtain the correlations, such as linear entropy of a single-qubit reduced state and a two-qubit entanglement measure, concurrence. We observe the variation of these correlations obtained from the experimental data with time and draw interesting observations, that are discussed in the main-text.